Journal of Inorganic Biochemistry 108 (2012) 22–29

Contents lists available at SciVerse ScienceDirect

Journal of Inorganic Biochemistry

journal homepage: www.elsevier.com/locate/jinorgbio

Synthesis, structures and urease inhibition studies of copper(II) and nickel(II) complexes with bidentate N,O-donor Schiff base ligands

Xiongwei Dong [a], Yuguang Li [a,b,*], Zuowen Li [a], Yongming Cui [a], Hailiang Zhu [b,**]

[a] School of Chemistry and Chemical Engineering, Wuhan Textile University, Wuhan 430073, PR China
[b] State Key Laboratory of Pharmaceutical Biotechnology, Nanjing University, Nanjing 210093, PR China

ARTICLE INFO

Article history:
Received 8 September 2011
Received in revised form 25 November 2011
Accepted 21 December 2011
Available online 29 December 2011

Keywords:
Copper(II) complexes
Schiff base ligands
X-ray structure
Urease inhibitors
Molecular docking

ABSTRACT

Five mononuclear copper(II) and nickel(II) complexes of Schiff base ligands derived from 4-hydroxyphenethylamine and 2-phenylethylamine were synthesized and determined by single crystal X-ray analysis. The crystal structures of these complexes presented the square planar coordination geometry at the metal center. The inhibitory activity of all the obtained complexes was tested in vitro against jack bean urease. It was found that Schiff base copper(II) complexes, namely $[Cu(C_{15}H_{13}BrNO_2)_2]\cdot 2(C_6H_7N)$ (**1**), $[Cu(C_{15}H_{12}Br_2NO_2)_2]\cdot 2(DMF)$ (**2**), $Cu(C_{19}H_{16}NO_2)_2$ (**3**) and $Cu(C_{19}H_{16}NO)_2$ (**5**), showed strong inhibitory activity against jack bean urease ($IC_{50}=1.45–3.59$ μM), while Schiff base nickel(II) complex, $[Ni(C_{19}H_{16}NO_2)_2]\cdot 2(DMF)$ (**4**), exhibited weak inhibitory activity ($IC_{50}>50$ μM). Their structure–activity relationships were further discussed.

1. Introduction

Urease (urea amidohydrolase; E.C.3.5.1.5) is a nickel-containing enzyme that catalyzes the rapid hydrolysis of urea to form ammonia and carbamate in a variety of algae, bacteria, fungi and plants [1–5]. It participates in environmental nitrogen transformations to supply these organisms with a nitrogen source for growth [3]. On the other hand, the reaction catalyzed by the dinuclear nickel active site of urease causes an accumulation of ammonia and an abrupt pH increase, which has negative side effects in agriculture and health. For example, urease serves as a virulence factor in pathogens that are responsible for the development of kidney stones, pyelonephritis, peptic ulcers, and other disease states [3,4]. In another context, urease can severely decrease the efficiency of urea fertilizers to cause the release of large amounts of ammonia and further induce plant damage by ammonia toxicity and soil pH increase [5]. Therefore, the capability to control the rate of the enzymatic urea hydrolysis using urease inhibitors is an important goal to pursue.

Recently, urease inhibition studies have attracted increasing attention [6–9] and the numerous urease inhibitors have also been reported [10–19]. Among the known inhibitors of urease, hydroxamic acids, phosphoramides and thiols are the best recognized urease inhibitors [10–13]. However, the discovery of new and more efficient inhibitors has so far relied upon extended screen tests because of the low efficiency and negative side effects of the presently available inhibitors against plant, bacterial and fungal ureases. In earlier studies, we have investigated the inhibition of jack bean urease by a series of Schiff base metal complexes and their urease inhibitory activity was found [20–22]. An interesting observation is that their reported biological activities are significantly influenced by metal center and the positions of the substituent groups such as halogen atoms in the aromatic ring. The full mechanism of the action is unclear yet. As a continuation of our work on Schiff base complexes as the urease inhibitor, the urease inhibitory activities of Schiff base copper(II) complexes **1**, **2**, **3** and **5**, and nickel(II) complex **4** were investigated and reported in this paper. Here, Schiff base ligands HL^1, HL^2 and HL^3 were obtained from the condensation of 4-hydroxyphenethylamine with 5-bromosalicyladehyde, 3,5-dibromosalicyladehyde and 2-hydroxy-1-naphthaldehyde, respectively, while ligand HL^4 was prepared from the reaction of 2-phenylethylamine with 2-hydroxy-1-naphthaldehyde (Scheme 1). A preliminary docking study was carried out using the DOCK program to gain an understanding of urease inhibitory activity of complexes **1**–**5** and their structure–activity relationships were also described within this paper.

2. Experimental section

2.1. Materials and physical measurements

Urease (from jack beans, type III, activity 22 units/mg solid), HEPES (Ultra) buffer and urea (Molecular Biology Reagent) were from Sigma. All other chemicals and solvents were purchased from Aldrich and

* Correspondence to: Y. Li, School of Chemistry and Chemical Engineering, Wuhan Textile University, Wuhan 430073, PR China. Tel./fax: +86 27 8761 1776.
** Corresponding author. Tel./fax: +86 27 8761 1776.
E-mail address: liyg2010@wtu.edu.cn (Y. Li).

0162-0134/$ – see front matter © 2011 Elsevier Inc. All rights reserved.
doi:10.1016/j.jinorgbio.2011.12.006

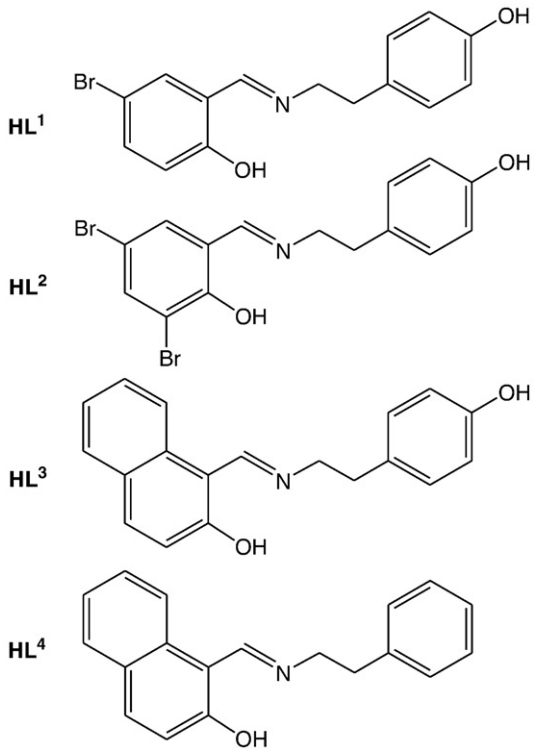

Scheme 1. The Schiff base ligands HL^1, HL^2, HL^3 and HL^4 used for the syntheses of complexes **1**–**5**.

used as received. Distilled water was used for all procedures. ^{1}H NMR spectra were recorded on a Bruker DRX-500 spectrometer. Chemical shifts were reported in ppm from tetramethylsilane as an internal standard (^{1}H, 0.00 ppm). Mass spectra were obtained on a Micromass GC–TOF for EI–MS (70 eV). Elemental analyses were performed using an elementar vario EL *III* elemental analyzer. Infrared spectra were obtained on a Nexus 870 FT-IR spectrophotometer using KBr pellets in the 4000–400 cm^{-1} range. UV–visible spectra were measured on a Shimadzu UV-160 A spectrophotometer using DMSO–H_2O (1:1 v/v) solvents in the 800–200 nm range. The enzyme inhibitory activity was measured on a Bio-Tek Synergy™ HT microplate reader.

2.2. General procedure for the synthesis of Schiff base ligands $HL^{1–4}$ (exemplified by HL^3)

4-Hydroxyphenethylamine (0.274 g, 2.0 mmol) was added to the solution of 2-hydroxy-1-naphthaldehyde (0.344 g, 2.0 mmol) in methanol (20 mL). The mixture was refluxed in methanol at 65 °C within 1 h. Subsequently, the solution was filtered and kept in air for about 7 days, to afford yellow block-shaped crystals of HL^3. Yield: 460 mg (79%), m.p. 197 °C dec. ^{1}H NMR (500 MHz, d_6-DMSO) δ: 13.99 (s, 1H), 9.20 (s, 1H), 8.99 (d, J = 10.5 Hz, 1H), 7.97–6.69 (m, 6H), 7.08 (d, J = 8.0 Hz, 2H), 6.67 (d, J = 8.0 Hz, 2H), 3.82 (t, 2H), 2.87 (t, 2H). EI–MS (70 eV): m/z 291 (M^+, 5%). IR (KBr, cm^{-1}): 3424, 2908, 2593, 1633, 1546, 1510, 1447, 1365, 1241, 1190, 1090, 855, 827, 748, 507, 487, 481, 435, 409. UV–visible [DMSO–H_2O (1:1 v/v), λ/nm (ε/M^{-1} cm^{-1})]: 416 (12,360), 400 (11,760), 308 (10,130), 268 (12,510), 262 (17,380), 252 (20,070). *Anal.* Calcd for $C_{19}H_{17}NO_2$: C, 78.33; H, 5.88; N, 4.81. Found: C, 78.11; H, 5.96; N, 4.60.

2.3. General method for the preparation of complexes 1–5

The Schiff base ligands $HL^{1–4}$ (1 mmol) were dissolved in the solvent mixture (10 mL) of methanol and N,N-dimethyl formamide (DMF) (1:1), respectively, which was added to $Cu(NO_3)_2 \cdot 3H_2O$ (0.5 mmol) in 4-methylpyridine (5 mL) or $Ni(NO_3)_2 \cdot 6H_2O$ (0.5 mmol) in methanol (5 mL). The resulting solution was stirred for 30 min at room temperature and then filtered. The filtrate was kept in air for about 7 days, forming block crystals. The crystals were isolated, washed three times with distilled water and dried in a vacuum desiccator containing anhydrous $CaCl_2$.

$$\left[Cu\left(L^1\right)_2\right] \cdot 2(4-\text{methylpyridine}) \quad (1)$$

Brown black solid, yield: 235 mg (53%). IR (KBr, cm^{-1}): 3447, 2901, 2599, 1618, 1516, 1460,1386, 1322, 1259, 1174, 1069, 1013, 823, 701, 648, 512, 484, 431. UV–visible [DMSO–H_2O (1:1 v/v), λ/nm (ε/M^{-1} cm^{-1})]: 370 (9,740), 294 (11,850), 258 (28,480). *Anal.* Calcd for $C_{42}H_{40}Br_2CuN_4O_4$: C, 56.80; H, 4.54; N, 6.31. Found: C, 56.96; H, 4.71; N, 6.10%.

$$\left[Cu\left(L^2\right)_2\right] \cdot 2(\text{DMF}) \quad (2)$$

Brown black solid, yield: 282 mg (56%). IR (KBr, cm^{-1}): 3422, 2929, 1664, 1620, 1513, 1446, 1384, 1321, 1243, 1157, 1102, 858, 826, 707, 669, 523, 489, 432. UV–visible [DMSO–H_2O (1:1 v/v), λ/nm (ε/M^{-1} cm^{-1})]: 376 (8,550), 268 (20,730), 256 (25,270). *Anal.* Calcd for $C_{36}H_{38}Br_4CuN_4O_6$: C, 42.99; H, 3.81; N, 5.57. Found: C, 42.76; H, 3.92; N, 5.31%.

$$\left[Cu\left(L^3\right)_2\right] \quad (3)$$

Brown black solid, yield: 200 mg (62%). IR (KBr, cm^{-1}): 3370, 3062, 2914, 2856, 1610, 1546, 1511, 1439, 1415, 1364, 1343, 1305, 1249, 1190, 1139, 1097, 1033, 965, 824, 748, 647, 603, 563, 524, 492, 463, 419. UV–visible [DMSO–H_2O (1:1 v/v), λ/nm (ε/M^{-1} cm^{-1})]: 414 (8,650), 396 (13,290), 380 (12,080), 310 (23,180), 262 (29,370). *Anal.* Calcd for $C_{38}H_{32}CuN_2O_4$: C, 70.85; H, 5.01; N, 4.35. Found: C, 70.71; H, 5.07; N, 4.28%.

$$\left[Ni\left(L^3\right)_2\right] \cdot 2(\text{DMF}) \quad (4)$$

Brownish yellow solid, yield: 188 mg (48%). IR (KBr, cm^{-1}): 3167, 3062, 2926, 2809, 1662, 1611, 1542, 1511, 1442, 1412, 1368, 1344, 1237, 1195, 1142, 1102, 1058, 1032, 970, 934, 826, 749, 664, 570, 534, 477, 421. UV–visible [DMSO–H_2O (1:1 v/v), λ/nm (ε/M^{-1} cm^{-1})]: 416 (7,280), 400 (7,410), 308 (8,920), 272 (16,850), 263 (17,730), 252 (19,710). *Anal.* Calcd for $C_{44}H_{46}NiN_4O_6$: C, 67.27; H, 5.90; N, 7.13. Found: C, 67.01; H, 5.97; N, 7.01%.

$$\left[Cu\left(L^4\right)_2\right] \quad (5)$$

Brown black solid, yield: 205 mg (67%). IR (KBr, cm^{-1}): 3444, 3025, 2907, 1612, 1540, 1500, 1462, 1410, 1365, 1202, 1091, 1027, 958, 825, 743, 696, 522, 499, 415. UV–visible [DMSO–H_2O (1:1 v/v), λ/nm (ε/M^{-1} cm^{-1})]: 420 (6,330), 400 (6,060), 312 (6,780), 248 (11,660). *Anal.* Calcd for $C_{38}H_{32}CuN_2O_2$: C, 74.55; H, 5.27; N, 4.58. Found: C, 74.43; H, 5.36; N, 4.33%.

2.4. Crystal structure determinations

X-ray crystallographic data [23,24] were collected on a Bruker SMART Apex II CCD diffractometer using graphite-monochromated Mo K_α (λ = 0.71073 Å) radiation. The collected data were reduced using the SAINT program, and empirical absorption corrections were performed using the SADABS program. The structures were solved by direct methods and refined against F^2 by full-matrix least-squares methods using the SHELXTL version 5.1. All of the non-hydrogen atoms were refined anisotropically. All other hydrogen atoms were placed in geometrically ideal positions and constrained

to ride on their parent atoms. The crystallographic data for the Schiff base ligands (HL^2, HL^3) and Schiff base metal complexes (**1**, **2**, **3**, **4** and **5**) are summarized in Tables 1 and 2.

2.5. Measurement of jack bean urease inhibitory activity

The measurement of urease activity was carried out according to the literature reported by Tanaka [25]. Generally, the assay mixture, containing 25 μL of jack bean urease (12 kU/L) and 25 μL of the tested complexes of different concentrations (dissolved in DMSO/H_2O mixture (1:1 v/v)), was preincubated for 1 h at 37 °C in a 96-well assay plate. After preincubation, 200 μL of 100 mM HEPES (N-[2-hydroxyethyl] piperazine-N′-[2-ethanesulfonic acid]) buffer [26] pH = 6.8 containing 500 mM urea and 0.002% phenol red were added and incubated at 37 °C. The reaction was measured by micro plate reader (570 nm), which was required to produce enough ammonium carbonate to raise the pH of a HEPES buffer from 6.8 to 7.7, the endpoint being determined by the color of phenol red indicator [27].

2.6. Docking simulations

Molecular docking of the inhibitor with the three-dimensional structure of jack bean urease (entry 3LA4 in the Protein Data Bank) was carried out using the DOCK 4.2 program suite [28–31]. The graphical user interface AutoDockTools (ADT 1.4.5) was performed to setup every inhibitor–enzyme interaction, where all hydrogen atoms were added, Gasteiger charges were calculated and nonpolar hydrogen atoms were merged to carbon atoms. The Ni initial parameters are set as $r = 1.170$ Å, $q = +2.0$, and van der Waals well depth of 0.100 kcal/mol [32]. As performed by the graphical user interface AutoDockTools, the catalytic center and the peripheral anionic site of the target protein were scanned to evaluate the modeled binding mode of the inhibitor–urease complex. The flexible docking of the ligand structures was done by the Lamarckian genetic algorithm (LGA), searching for favorable bonding conformations of the ligands at the sites of the target protein. The docking procedure of Schiff base copper(II) complexes **1**, **2**, **3** and **5** with the enzyme active site of jack bean urease was performed as described previously by our group [33,34].

3. Results and discussion

3.1. Synthesis

Condensation of salicylaldehydes or salicylaldehyde derivatives with primary amines leads to the formation of an important class of the bidentate Schiff base ligands. The Schiff base ligands HL^1, HL^2 and HL^3 were prepared by the reaction of 4-hydroxyphenethylamine with the corresponding 5-bromosalicylaldehyde, 3,5-dibromosalicyl-aldehyde and 2-hydroxy-1-naphthaldehyde in nearly 70–80% yield in methanol, while the ligand HL^4 was obtained by the reaction of 2-phenylethylamine with 2-hydroxy-1-naphthaldehyde. These Schiff base ligands are the stable solids and can be stored without precautions. In general, Schiff base ligands HL^{1-4} may dissolve in the polar solvent such as methanol and N,N-dimethyl formamide (DMF). Treatment of the Schiff base ligands HL^{1-4} with the respective metal salt, $Cu(NO_3)_2 \cdot 3H_2O$ and $Ni(NO_3)_2 \cdot 6H_2O$, in a 2:1 M ratio at ambient temperature led to the copper(II) complexes **1**, **2**, **3** and **5**, and nickel(II) complex **4**. Crystals of complexes **1**–**5** suitable for X-ray diffraction could be isolated from 4-methylpyridine/methanol or DMF/methanol after slow evaporation of the solvent over a period of a week. The spectroscopic data is in good agreement with the chemical formula proposed for Schiff base complexes **1**–**5**.

3.2. Spectroscopic studies (Supplementary data)

On the basis of the structure found and a comparison with spectra of related complexes [35–37], the IR spectra of complexes **1**–**5** have been tentatively assigned. The broadness of the ν(O–H) band between 3447 and 3167 cm^{-1} may be attributed to the phenolic hydroxyl

Table 2
Crystal data for HL^2, HL^3 and complexes **1**–**5**.

Compound	HL^2	HL^3
Empirical formula	$C_{15}H_{13}Br_2NO_2$	$C_{19}H_{17}NO_2$
Molecular weight	399.08	291.34
Crystal system	Orthorhombic	Orthorhombic
Space group	$P2_12_12_1$	*Pbca*
a (Å)	8.1072(16)	12.5136(17)
b (Å)	8.8634(17)	11.4059(16)
c (Å)	21.038(4)	20.092(3)
α (°)	90	90
β (°)	90	90
γ (°)	90	90
T (K)	298(2)	291(2)
V (Å^3)	1511.7(5)	2867.7(7)
Z	4	8
$\rho_{calc.}$ (g·cm^{-3})	1.754	1.350
F(000)	784	1232
μ(Mo-K$_\alpha$) (mm^{-1})	5.362	0.088
Data/restraint/parameters	2958/0/182	2527/0/203
Goodness-of-fit on F^2	1.003	1.001
Final R_1, wR_2 [$I > 2\sigma(I)$]	0.0364/0.0716	0.0634/0.0790

Table 1
Crystal data for HL^2, HL^3 and complexes **1**–**5**.

Complex	1	2	3	4	5
Empirical formula	$C_{42}H_{40}Br_2CuN_4O_4$	$C_{36}H_{38}Br_4CuN_4O_6$	$C_{38}H_{32}CuN_2O_4$	$C_{44}H_{46}N_4NiO_6$	$C_{38}H_{32}CuN_2O_2$
Molecular weight	888.14	1005.88	644.20	785.56	612.20
Crystal system	Monoclinic	Triclinic	Triclinic	Monoclinic	Triclinic
Space group	*C*2/*c*	*P* − 1	*P* − 1	$P2_1/c$	*P* − 1
a (Å)	38.069(3)	6.2178(6)	9.069(2)	18.276(2)	5.1785(3)
b (Å)	5.7043(5)	9.2270(11)	10.030(2)	10.2304(12)	15.8614(10)
c (Å)	19.7619(16)	18.1787(18)	10.157(2)	11.0151(13)	18.1411(11)
α (°)	90.00	78.042(2)	67.743(4)	90.00	90.2320(10)
β (°)	114.206(2)	84.892(2)	63.737(4)	106.473(2)	96.6460(10)
γ (°)	90.00	70.359(2)	69.342(5)	106.473(2)	93.4460(10)
T (K)	298(2)	291(2)	298(2)	291(2)	298(2)
V (Å^3)	3914.1(6)	960.73(18)	747.5(3)	1975.0(4)	1477.30(15)
Z	4	1	1	2	2
$\rho_{calc.}$ (g·cm^{-3})	1.507	1.739	1.431	1.321	1.376
F(000)	1804	499	335	828	638
μ(Mo-K$_\alpha$) (mm^{-1})	2.646	4.777	0.777	0.545	0.777
Data/restraint/parameters	3825/0/243	3762/26/235	2898/0/206	3874/0/253	5718/0/391
Goodness-of-fit on F^2	1.009	1.003	0.943	1.002	1.003
Final R_1, wR_2 [$I > 2\sigma(I)$]	0.0450, 0.1046	0.0329, 0.0894	0.0660, 0.0793	0.0485, 0.1116	0.0364, 0.0836

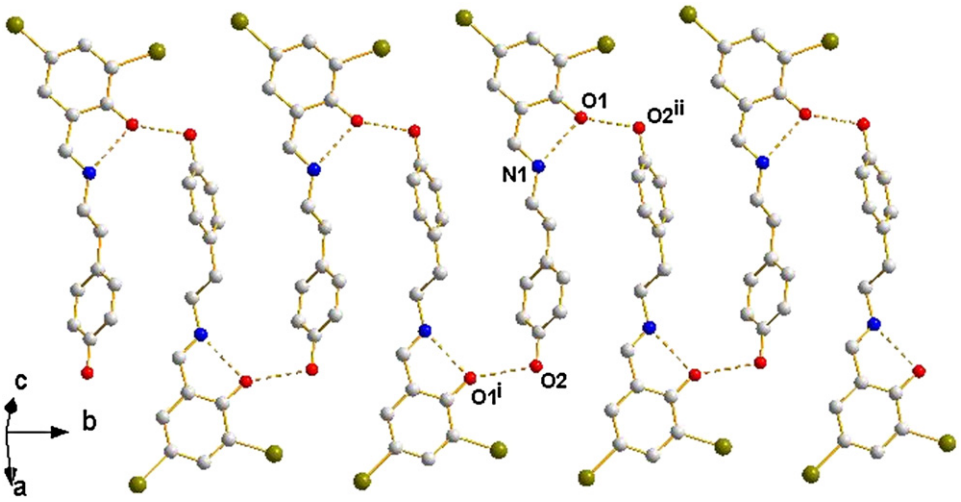

Fig. 1. One-dimensional zigzag chain structure of HL^2. (symmetry codes: (i) $1-x, -1/2+y, 1/2-z$; (ii) $1-x, 1/2+y, 1/2-z$).

group of complexes **1**–**5**. The IR spectra of complexes **1**–**5** exhibit strong absorption between 1620 and 1610 cm^{-1}, assignable to the ν(C═N) absorption. It can be observed that the ν(C═N) vibration band suffers a negative shift in complexes **2** and **3** with respect to the corresponding free ligand HL^2 and HL^3 at 1643 and 1633 cm^{-1}, thus indicating that the imine nitrogen atom is involved in coordination to the metal ion. The appearances of the strong absorption at 1664 and 1662 cm^{-1} in **2** and **4** were attributed to the ν(C═O) absorption of the lattice DMF molecule. The broad strong absorption between 1546 and 1500 cm^{-1} in all complexes could be reasonably attributed to the presence of the ν(C═C) stretching vibration of the aromatic ring backbone. The UV–vis spectra for the Schiff base complexes **1**–**5** were obtained in assay conditions (DMSO/H_2O, 1:1 v/v). The electronic spectra of the Schiff base copper(II) complexes **1** and **2** are very similar and show the moderately intense UV band near 370 nm originating from a phenolate to metal ion charge-transfer [38,39]. The absorption maxima of complex **2** are blue-shifted compared to **1**, probably because of the acceptor effect of the 3-bromine substituent. In the electronic spectra of complexes **3**, **4** and **5**, the intense higher-energy bands at around 260 nm are attributed to an intraligand charge transfer ($\pi \rightarrow \pi^*$). The formation of complexes **3** and **5** in DMSO/H_2O mixture is supported by the strong and broad charge-transfer band at 310 and 312 nm, and also by the evolution of a shoulder in the close UV range between 380 and 420 nm, originated from a charge transfer band. The shoulder centered at 388 nm in the UV–vis spectrum of **3** is blue-shifted relative to its free ligand HL^3. Similar spectra are observed for Schiff base nickel(II) complex **4** and its free ligand HL^3, whereas **4** exhibits somewhat weaker absorption bands appeared at 308 nm, 400 nm, 416 nm than the corresponding HL^3 ligand. In the electronic spectra of all complexes **1**–**5**, bands associated with $d \rightarrow d$ transitions were not detected, perhaps due to the intensity of the charge transfer and intraligand transitions [40].

3.3. Crystal structure description

The study shows that the Schiff base ligands HL^1, HL^2, HL^3 and HL^4 are much alike (Scheme 1). These bidentate N,O-donor ligands are able to coordinate as a monoanionic species through their deprotonated phenolic hydroxyl groups. Analogous N,O-bidentate chelating Schiff base species has been obtained from the condensation of salicylaldehyde with 4-hydroxyphenethylamine in our group [41]. Unfortunately, the Schiff base ligands HL^1 and HL^4 could not be crystallized in a form suitable for X-ray single crystal diffraction studies and thus only the crystal structures of HL^2 and HL^3 have been determined. The solid-state structures of the Schiff base ligands HL^2 and HL^3 are shown in Figs. 1 and 2. In the ligands HL^2 and HL^3 derived from 3,5-dibromosalicylaldehyde and 2-hydroxy-1-naphthaldehyde, the C═N bond distances are 1.286(6) and 1.307(3) Å, respectively. Interestingly, the Schiff base ligands HL^2 and HL^3 were linked into a zigzag chain by the intramolecular O–H···N hydrogen bonds and the intermolecular O–H···O hydrogen bonds between the corresponding adjacent molecules [O1···N1 2.553(4) Å, O2···O1# 2.720(4) Å for HL^2; O1···N1 2.592(3), O2···O1# 2.662(3) Å for HL^3].

The Schiff base metal complexes **1**–**5** with general formula $M(L)_2$, where $L = L^1$, L^2, L^3 and L^4, were obtained from the combination of two equivalents of the Schiff base ligands HL^{1-4} with a metal ion ($M = Cu^{2+}$, Ni^{2+}). The molecular structures of complexes **1**–**5** were determined by single crystal X-ray analysis as shown in Figs. 3–7. All five complexes afford the square planar coordination geometry,

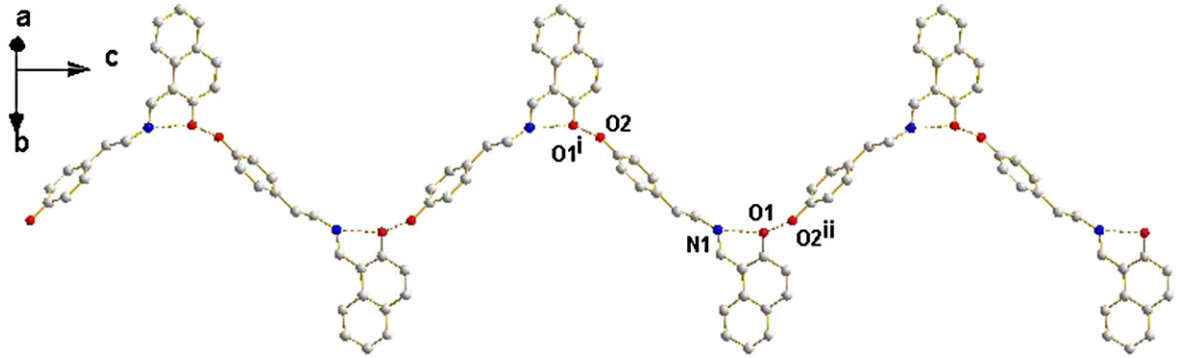

Fig. 2. One-dimensional zigzag chain structure of HL^3. (symmetry codes: (i) $3/2-x, -y, -1/2+z$; (ii) $3/2-x, -y, 1/2+z$).

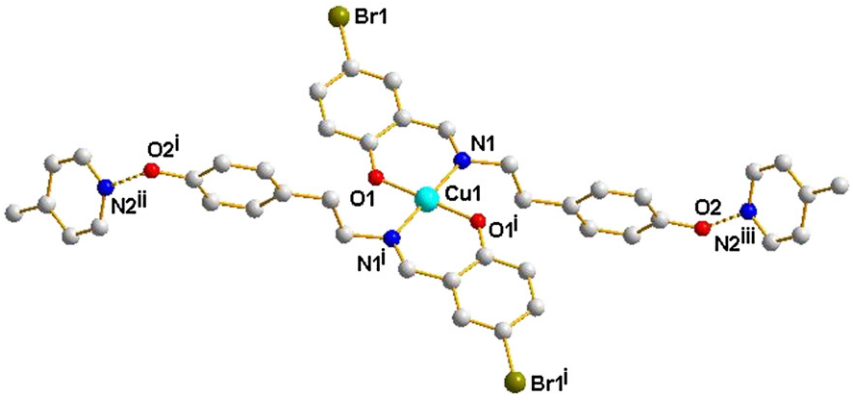

Fig. 3. *Ball-and-stick* representation of the molecular structure of **1** (symmetry codes: (i) 1/2 − *x*, 5/2 − *y*, −*z*; (ii) 1/2 − *x*, 5/2 + *y*, 1/2 − *z*; (iii) *x*, −*y*, −1/2 + *z*), atoms are shown as sphere of arbitrary diameter.

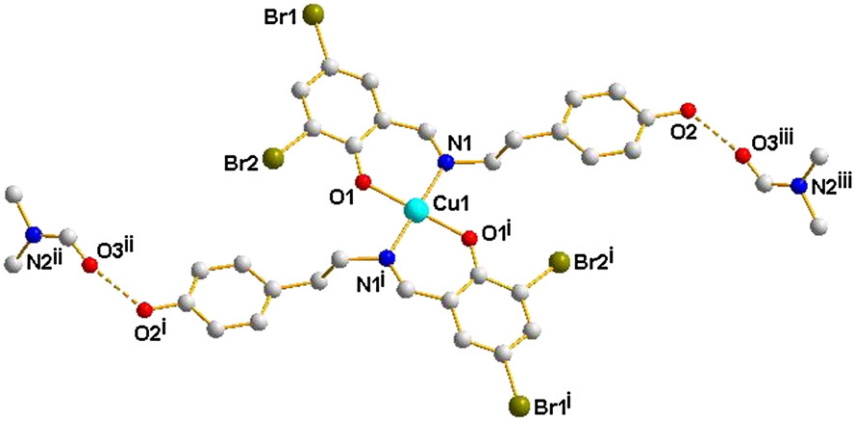

Fig. 4. *Ball-and-stick* representation of the molecular structure of **2** (symmetry codes: (i) 1 − *x*, −*y*, 1 − *z*; (ii) 2 − *x*, −*y*, −*z*; (iii) −1 + *x*, *y*, 1 + *z*), atoms are shown as sphere of arbitrary diameter.

where the metal ion is four-coordinated by two imine N atoms and two phenolic O atoms from two Schiff base ligands (L) in a *trans* position. Selected bond distances and bond angles at the metal center for complexes **1**–**5** are listed in Table 3. Single crystal X-ray diffraction reveals that Schiff base copper(II) complexes **1** and **2** crystallize in the monoclinic *C*2/c (No. 15) space group and triclinic *P*-1 (No. 2) space group, respectively. As depicted in Figs. 3 and 4, complexes **1** and **2** are the mononuclear copper(II) species with formula $[Cu(L^1)_2]\cdot 2$(4-methylpyridine) and $[Cu(L^2)_2]\cdot 2$DMF, to afford the square planar *trans*-$[CuN_2O_2]$ coordination geometry, where the Cu(II) atom lies on a center-of-inversion. The average Cu – O and Cu – N bond distances of 1.882(2) and 2.004(2) Å in complex **1** are slightly shorter than that of 1.906(2) and 2.010(2) Å observed in **2**, respectively, probably due to the electron withdrawing effect of the bromine substituent. This suggests that the position of the bromine atom in the aromatic ring has significant effect on the coordination abilities of the ligands [39]. The $Cu(L^1)_2$ moiety in the crystal structure of **1** is linked with two co-crystallized 4-methylpyridine solvent molecules through the intermolecular O2 – H2···N2 hydrogen bonds [O2···N2 2.713(5) Å] (Fig. 3), while the $Cu(L^2)_2$ moiety in **2** is connected with two DMF molecules through the intermolecular O2 – H2···O3 hydrogen bonds [O2···O3 2.588(8) Å] (Fig. 4).

The X-ray crystal structure reveals that complexes **3** and **4** are the mononuclear copper(II) and nickel(II) species of formula $Cu(L^3)_2$ and $[Ni(L^3)_2]\cdot 2$DMF, respectively (Figs. 5 and 6). These two complexes have the same bidentate backbone of the chelate Schiff base ligand HL^3 and the same metal coordination spheres. In contrast to complex **3**, the crystal structure of **4** consists of a discrete mononuclear $Ni(L^3)_2$ unit and two lattice DMF molecules. The coordination geometry of the nickel(II) atom in the $Ni(L^3)_2$ unit closely resembles that observed for complex **3**. Analogous copper(II) and nickel(II) species of Schiff base ligands derived from 4-hydroxyphenethylamine have been reported by our group [20]. The bond distances of Ni1 – O1 and Ni1 – N1 are 1.825 (2) and 1.911(2) Å, which are comparable with the corresponding values reported for analogous square planar Ni(II) species [20,36,42]. The $Ni(L^3)_2$ moiety in **4** is further connected with two DMF molecules through the intermolecular O2 – H2···O3 hydrogen

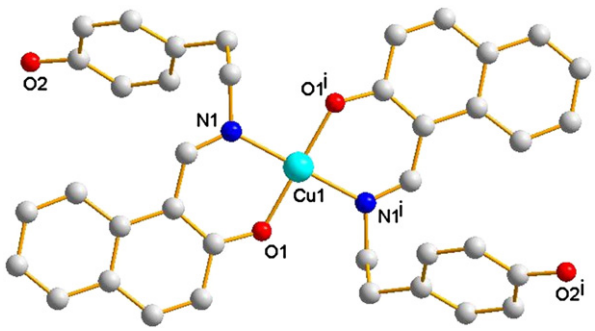

Fig. 5. *Ball-and-stick* representation of the molecular structure of **3** (symmetry code: (i) 1 − *x*, 1 − *y*, 1 − *z*), atoms are shown as sphere of arbitrary diameter.

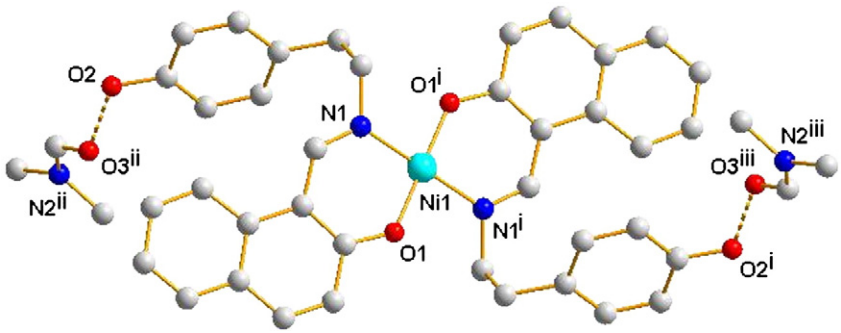

Fig. 6. *Ball-and-stick* representation of the molecular structure of **4** (symmetry codes: (i) $1-x, 1-y, -z$; (ii) $-x, 1-y, -z$; (iii) $1+x, y, z$), atoms are shown as sphere of arbitrary diameter.

bonds [O2···O3 2.663(3) Å] (Fig. 6). In contrast to complexes **1**–**3**, the solid-state structure of the Schiff base copper(II) complex **5** derived from 2-phenylethylamine contains two crystallographically independent molecules. The molecular structure of one of the two rather similar complex units, $Cu(L^4)_2$, is represented in Fig. 7. The copper(II) atom in each mononuclear $Cu(L^4)_2$ unit of **5** also lies on a crystallographic inversion center (symmetry codes: $1-x, 1-y, 1-z$ for Cu1; $1-x, 2-y, -z$ for Cu2). The average bond distances of Cu1–O1 and Cu1–N1 are 1.879(2) and 1.998(2) Å, respectively, while the average bond distances of Cu2–O2 and Cu2–N2 are 1.881(2) and 2.006(2) Å.

3.4. Inhibitory activity against jack bean urease

The Schiff base ligands HL^{1-4} and the corresponding copper(II) **1**, **2**, **3** and **5** and nickel(II) complex **4** were screened for inhibitory activity against jack bean urease (see Table 4). It was found that all the synthesized ligands HL^1, HL^2, HL^3 and HL^4 exhibited no ability to inhibit the jack bean urease. Compared with the standard inhibitor acetohydroxamic acid (AHA, $IC_{50} = 63.00$ μM), the Schiff base copper(II) complexes **1**, **2**, **3** and **5** displayed potent inhibitory activity against jack bean urease. Generally, heavy metal ions are believed to inhibit the urease by binding to the sulfhydryl groups of cysteines, and possibly nitrogen-(histidine) and oxygen-(aspartic and glutamic acids) in the urease active site [43–46]. Thus it can be seen that coordination to copper(II) ion resulted in the improved inhibitory activity [47–49]. It should be noted that in terms of the inhibitory strength towards jack bean urease the Schiff base copper(II) complexes studied form the order: **3** > **1** > **2** > **5**. Here, complex **1** is more potent than complex **2** as a result of the difference of the electron-withdrawing bromine substituent on the aromatic ring. Interestingly, complex **3** derived from 4-hydroxyphenethylamine is much more potent than complex **5** derived from 2-phenylethylamine. This defines the minimal substitution patterns in the aromatic ring for obtaining the potent activity. Among the four Schiff base copper(II) complexes **1**, **2**, **3** and **5** tested, the most potent activity was observed in complex **3** only. These observations are in agreement with the previously reported Schiff base copper(II) complexes derived from 4-hydroxyphenethylamine [20]. When compared with complex **3**, the Schiff base nickel(II) complex **4** exhibits weaker urease inhibitory activity ($IC_{50} = 52$ μM) under the same condition. The results indicate that inhibitory activities of Schiff base metal complexes as the urease inhibitor depend on not only the organic ligands but also the central ions.

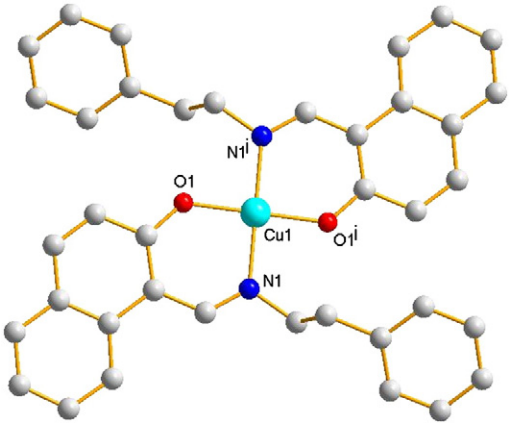

Fig. 7. *Ball-and-stick* representation of the molecular structure of **5** (symmetry code: (i) $1-x, 1-y, 1-z$), atoms are shown as sphere of arbitrary diameter.

3.5. Molecular docking study

The binding models of Schiff base copper(II) complexes **1**, **2**, **3** and **5** with jack bean urease were simulated using the Dock program to validate their structure–activity relationships (Fig. 8) [28–31]. The results revealed that the complex molecules were well filled in the active pocket of jack bean urease. Additional interactions have been established in a variety of conformations because of the flexibilities of the chelating phenolic oxygen atom and the amino acid residues

Table 3
Selected bond lengths (Å) and angles (°) for complexes **1**–**5**.

1 (i = 1/2 − x, 5/2 − y, −z)			
Cu(1)–O(1)	1.882(2)	O(1)–Cu(1)–N(1)	91.57(10)
Cu(1)–O(1)^{i}	1.882(2)	O(1)^{i}–Cu(1)–N(1)	88.43(10)
Cu(1)–N(1)	2.004(2)	O(1)–Cu(1)–O(1)^{i}	180.0
Cu(1)–N(1)^{i}	2.004(2)		
2 (i = 1 − x, -y, 1 − z)			
Cu(1)–O(1)	1.906(2)	O(1)–Cu(1)–N(1)	91.70(9)
Cu(1)–O(1)^{i}	1.906(2)	O(1)^{i}–Cu(1)–N(1)	88.29(9)
Cu(1)–N(1)	2.010(2)	O(1)–Cu(1)–O(1)^{i}	179.999(1)
Cu(1)–N(1)^{i}	2.010(2)		
3 (i = 1 − x, 1 − y, 1 − z)			
Cu(1)–O(1)	1.900(3)	O(1)–Cu(1)–N(1)	90.27(12)
Cu(1)–O(1)^{a}	1.900(3)	O(1)^{a}–Cu(1)–N(1)	89.73(12)
Cu(1)–N(1)	1.987(3)	O(1)–Cu(1)–O(1)^{a}	180.000(1)
Cu(1)–N(1)^{a}	1.987(3)		
4 (i = 1 − x, 1 − y, −z)			
Ni(1)–O(1)	1.8255(16)	O(1)–Ni(1)–N(1)	87.82(8)
Ni(1)–O(1)^{i}	1.8255(16)	O(1)^{i}–Ni(1)–N(1)	92.18(8)
Ni(1)–N(1)	1.911(2)	O(1)–Ni(1)–O(1)^{i}	180.000(2)
Ni(1)–N(1)^{i}	1.911(2)		
5 (i = 1 − x, 1 − y, 1 − z; ii = 1 − x, 2 − y, −z)			
Cu(1)–O(1)	1.8793(14)	O(1)–Cu(1)–N(1)	90.84(6)
Cu(1)–O(1)^{i}	1.8793(14)	O(1)^{i}–Cu(1)–N(1)	89.16(6)
Cu(1)–N(1)	1.9981(16)	O(1)–Cu(1)–O(1)^{i}	179.999(1)
Cu(1)–N(1)^{i}	1.9981(16)	Cu(2)–N(2)^{ii}	2.0055(16)
Cu(2)–O(2)	1.8814(14)	O(2)–Cu(2)–N(2)	90.53(6)
Cu(2)–O(2)^{ii}	1.8814(14)	O(2)^{ii}–Cu(2)–N(2)	89.47(6)
Cu(2)–N(2)	2.0055(16)	O(2)–Cu(2)–O(2)^{ii}	180.0

Table 4
Inhibition of jack bean urease by Schiff base ligands and complexes **1**–**5**.

Tested materials	IC_{50} (μM)
HL^{1-4}	>100
1	2.80
2	3.22
3	1.45
4	52.00
5	3.59
Acetohydroxamic acid	63.00

of jack bean urease. The optimized cluster (20 occurrences) was ranked by energy level in the best conformation of the inhibitor–urease modeled structures, where the binding energy of the amino acid residues with the corresponding copper(II) complexes **1**, **2**, **3** and **5** shows −7.60 kcal/mol, −6.62 kcal/mol, −3.64 kcal/mol, −3.36 kcal/mol, and the lowest intermolecular energy presents −9.79 kcal/mol, −8.81 kcal/mol, −5.84 kcal/mol, −5.70 kcal/mol, respectively. Besides, some hydrophobic interactions also exist in the corresponding inhibitor–urease complex.

The binding modes of complexes **1** and **2** in the enzyme active site were modeled as depicted in Fig. 8a and b. It should be noted that the phenolic O atom of complexes **1** and **2** forms one hydrogen bond with the side chain N–H of Arg439, respectively. The hydrogen-bonding distance and angle of Arg439 $N-H\cdots O_{complex\text{-}1}$ are 2.652(2) Å and 140.8(2)°, while that of Arg439 $N-H\cdots O_{complex\text{-}2}$ are 2.907(2) Å and 143.0(2)°. This is due to the presence of a different bromine substituent in the aromatic ring of **1** and **2** derived from 4-hydroxyphenethylamine. In the inhibitor–urease complex structures, both **1** and **2** form some hydrophobic interactions with the amino acid residues such as Ala440 and Met637, and other intermolecular interactions with the amino acid residues such as His407, His409, His492, His593 and Asp633. In addition, the distances between two nickel(II) atoms in the active site of urease and the respective copper(II) atom of complexes **1** and **2** were calculated (9.030(2) and 9.002(2) Å for complex **1**; 8.971(2) and 8.703(2) Å for complex **2**).

In the best docking conformation (Fig. 8c), as expected, the aromatic ring of complex **3** was stacked against the imidazole and carbonyl moieties of His492, Asp494, His519, His593 and Ala636, respectively. The phenolic OH group of complex **3** derived from 4-hydroxyphenethylamine forms one hydrogen bond with the carboxylate group of Asp494. The hydrogen-bonding distance and angle of Asp494 $O\cdots H-O_{complex\text{-}3}$ are 2.422(2) Å and 156.9(2)°, respectively. In contrast, no hydrogen bond was found between complex **5** derived from 2-phenylethylamine and the amino acid residues of the urease active site (Fig. 8d). This probably causes the activity difference of complexes **3** and **5** as urease inhibitors. In addition, as a result of the strong intermolecular hydrogen bond formed between the chelating Schiff base ligand and the active site of the enzyme, the binding energy (−3.64 kcal/mol) and the lowest intermolecular energy (−5.84 kcal/mol) in the modeled structure of **3**-urease complex are slightly lower than the corresponding values (−3.36 kcal/mol and −5.70 kcal/mol) observed in the **5**-urease complex. The results further demonstrate exceptional difference of urease inhibitory activity of these copper(II) complexes.

4. Conclusion

This paper describes the synthesis, crystal structures and urease inhibitory activities of five new Schiff base copper(II) and nickel(II) complexes with the bidentate N,O-donor Schiff base ligands. It was found that this class of complexes exhibited strong inhibitory activity

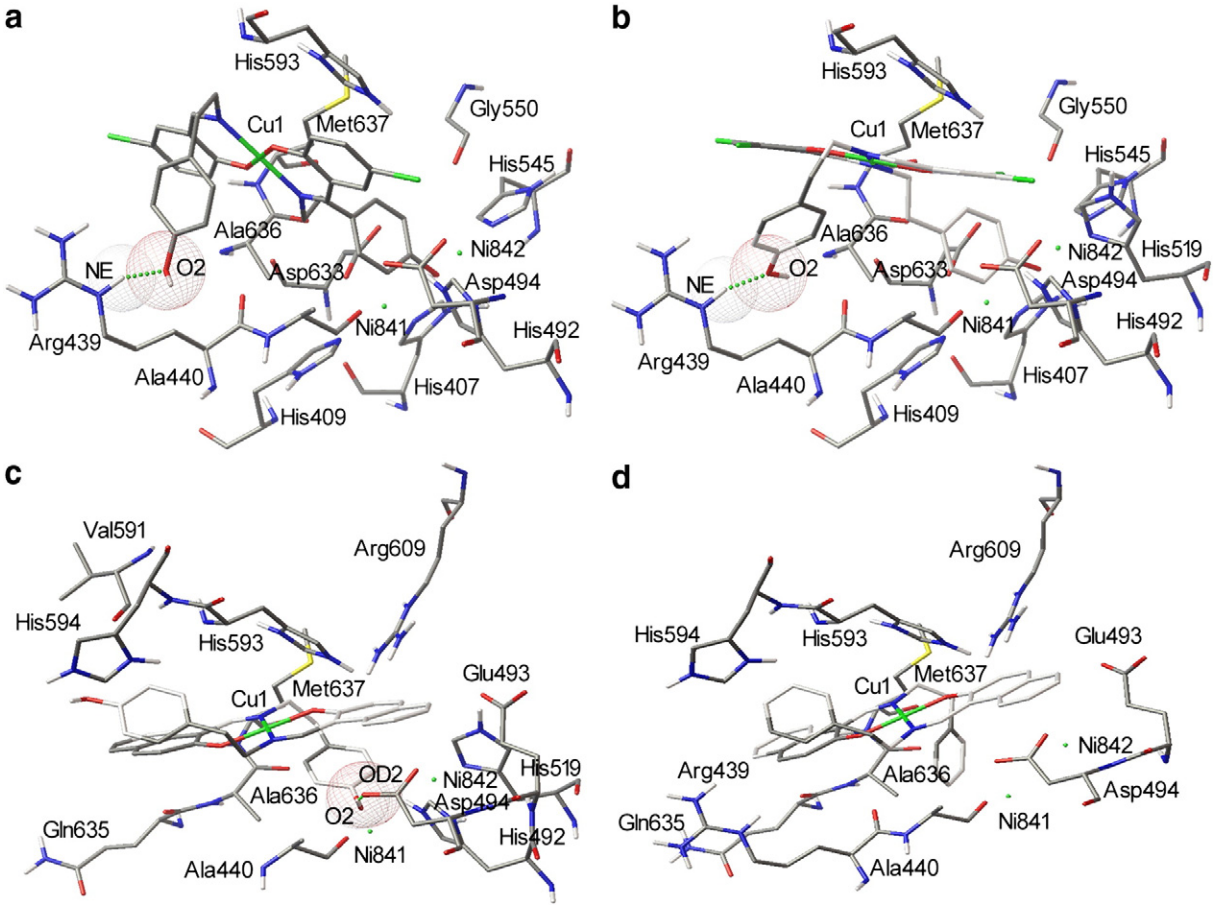

Fig. 8. Modeled structures of complexes of designed inhibitors **1** (a), **2** (b), **3** (c) and **5** (d) with jack bean urease. Hydrogen bonds are presented as green dotted lines.

against jack bean urease, while the copper(II) complex **3** afforded increased in vitro inhibitory activity ($IC_{50} = 1.45$ μM). The trend in this work is in accord with the studies reported earlier. The docking simulation described here suggests that Schiff base copper(II) species have good potential as the urease inhibitor in the future. Detailed investigations are continuing to study the mechanisms of urease inhibitory activity reported here.

Acknowledgments

This work was financially supported by the National Natural Science Foundation of China (21101122), China Postdoctoral Science Foundation (20100481108), Natural Science Foundation of Hubei Province (2009CDA022), and the Education Office of Hubei Province (Q20101610).

Appendix A. Supplementary data

CCDC numbers 823531–823537 contain the supplementary crystallographic data (CIF) for this article. These data can be obtained free of charge via http://www.ccdc.cam.ac.uk/conts/retrieving.html, or from the Director, CCDC, 12 Union Road, Cambridge CB2 1EZ, UK (Fax: +44-1223-336-033; e-mail: deposit@ccdc.cam.ac.uk). Supplementary materials related to this article can be found online at doi:10.1016/j.jinorgbio.2011.12.006.

References

[1] P.A. Karplus, M.A. Pearson, R.P. Hausinger, Acc. Chem. Res. 30 (1997) 330–337.
[2] R.P. Hausinger, Biochemistry of Nickel, Plenum Press, New York, 1993, pp. 23–57.
[3] H.L.T. Mobley, R.P. Hausinger, Microbiol. Rev. 53 (1989) 85–108.
[4] H.L.T. Mobley, M.D. Island, R.P. Hausinger, Microbiol. Rev. 59 (1995) 451–480.
[5] E. Jabri, M.B. Carr, R.P. Hausinger, P.A. Karplus, Science 268 (1995) 998–1004.
[6] S. Ciurli, S. Benini, W.R. Rypniewski, K.S. Wilson, S. Miletti, S. Mangani, Coord. Chem. Rev. 190–192 (1999) 331–355.
[7] D.I. Metelitza, E.I. Tarun, A.V. Puchkaev, Yu.P. Losev, Prikl. Biokhim. Mikrobiol. 37 (2001) 190–196.
[8] B. Krajewska, W. Zaborska, Bioorg. Chem. 35 (2007) 355–365.
[9] C. Follmer, J. Clin. Pathol. 63 (2010) 424–430.
[10] B. Krajewska, J. Mol, Catal. B Enzym. 59 (2009) 9–21.
[11] S. Vassiliou, P. Kosikowska, A. Grabowiecka, A. Yiotakis, P. Kafarski, Ł. Berlicki, J. Med. Chem. 53 (2010) 5597–5606.
[12] M. Font, M.-J. Domínguez, C. Sanmartín, J.A. Palop, S. San-Francisco, O. Urrutia, F. Houdusse, J.M. García-Mina, J. Agric. Food Chem. 56 (2008) 8451–8460.
[13] M.-J. Domínguez, C. Sanmartín, M. Font, J.A. Palop, S. San-Francisco, O. Urrutia, F. Houdusse, J.M. García-Mina, J. Agric. Food Chem. 56 (2008) 3721–3731.
[14] S. Benini, W.R. Rypniewski, K.S. Wilson, S. Ciurli, S. Mangani, J. Biol. Inorg. Chem. 6 (2001) 778–790.
[15] S. Benini, W.R. Rypniewski, K.S. Wilson, S. Mangani, S. Ciurli, J. Am. Chem. Soc. 126 (2004) 3714–3715.
[16] M.J. Todd, R.P. Hausinger, Biochemistry 39 (2000) 5389–5396.
[17] S. Vassiliou, A. Grabowiecka, P. Kosikowska, A. Yiotakis, P. Kafarski, Ł. Berlicki, J. Med. Chem. 51 (2008) 5736–5744.
[18] S. Benini, W.R. Rypniewski, K.S. Wilson, S. Ciurli, S. Mangani, J. Biol. Inorg. Chem. 3 (1998) 268–273.
[19] M.J. Todd, R.P. Hausinger, J. Biol. Chem. 264 (1989) 15835–15842.
[20] Y. Li, D.-H. Shi, H.-L. Zhu, H. Yan, S.W. Ng, Inorg. Chim. Acta 360 (2007) 2881–2889.
[21] W. Chen, Y. Li, Y. Cui, X. Zhang, H.-L. Zhu, Q. Zeng, Eur. J. Med. Chem. 45 (2010) 4473–4478.
[22] D.-H. Shi, Z.-L. You, C. Xu, Q. Zhang, H.-L. Zhu, Inorg. Chem. Commun. 10 (2007) 404–406.
[23] Bruker, SMART (Version 5.63), SAINT (Version 6.02), SADABS (Version 2.03), Bruker AXS Inc, Madison, WI, 2000.
[24] G.M. Sheldrick, Acta Crystallogr. A 64 (2008) 112–122.
[25] T. Tanaka, M. Kawase, S. Tani, Life Sci. 73 (2003) 2985–2990.
[26] W. Zaborska, B. Krajewska, Z. Olech, J. Enzyme, Inhib. Med. Chem. 19 (2004) 65–69.
[27] D.D. Van Slyke, R.M. Archibald, J. Biol. Chem. 154 (1944) 623–642.
[28] R. Huey, G.M. Morris, A.J. Olson, D.S. Goodsell, J. Comput. Chem. 28 (2007) 1145–1152.
[29] A. Balasubramanian, K. Ponnuraj, J. Mol. Biol. 400 (2010) 274–283.
[30] G. Estiu, D. Suárez, K.M. Merz, J. Comput. Chem. 27 (2006) 1240–1262.
[31] K. Takishima, T. Suga, G. Mamiya, Eur. J. Biochem. 175 (1988) 151–165.
[32] F. Musiani, E. Arnofi, R. Casadio, S. Ciurli, J. Biol. Inorg. Chem. 6 (2001) 300–314.
[33] Y.-M. Cui, Y. Li, Y.-J. Cai, W. Chen, H.-L. Zhu, J. Coord. Chem. 64 (2011) 610–616.
[34] Y.-M. Cui, W. Yan, Y.-J. Cai, W. Chen, H.-L. Zhu, J. Coord. Chem. 63 (2010) 3706–3713.
[35] R. Klement, F. Stock, H. Elias, H. Paulus, P. Pelikán, M. Valko, M. Mazúr, Polyhedron 18 (1999) 3617–3628.
[36] T. Akitsu, Y. Einaga, Polyhedron 24 (2005) 1869–1877.
[37] M. Kettunen, A.S. Abu-Surrah, H.M. Abdel-Halim, T. Repo, M. Leskelä, M. Laine, I. Mutikainen, M. Ahlgren, Polyhedron 23 (2004) 1649–1656.
[38] T. Szabó-Plánka, B. Gyurcsik, N.V. Nagy, A. Rockenbauer, R. Šípoš, J. Šima, M. Melník, J. Inorg. Biochem. 102 (2008) 101–109.
[39] T. Szabó-Plánka, B. Gyurcsik, I. Pálinkó, N.V. Nagy, A. Rockenbauer, R. Šípoš, J. Šima, M. Melník, J. Inorg. Biochem. 105 (2011) 75–83.
[40] I. Castillo, J.M. Fernández-González, J.L. Gárate-Morales, J. Mol. Struct. 657 (2003) 25–35.
[41] Y. Li, H.-L. Zhu, W.-Q. Huang, L. Ai, Acta Crystallogr. E 62 (2006) o689–o690.
[42] J.M. Fernández-G, M.J. Rosales-Hoz, M.F. Rubio-Arroyo, R. Salcedo, R.A. Toscano, A. Vela, Inorg. Chem. 26 (1987) 349–357.
[43] B. Krajewska, J. Enzyme. Inhib. Med. Chem. 23 (2008) 535–542.
[44] B. Krajewska, W. Zaborska, M. Chudy, J. Inorg. Biochem. 98 (2004) 1160–1168.
[45] W. Zaborska, B. Krajewska, M. Leszko, Z. Olech, J. Mol. Catal. B: Enzym. 13 (2001) 103–108.
[46] C. Follmer, C.R. Carlini, Arch. Biochem. Biophys. 435 (2005) 15–20.
[47] W.H.R. Shaw, D.N. Raval, J. Am. Chem. Soc. 83 (1961) 3184–3187.
[48] X. Dong, Y. Li, Z. Li, D. Gong, H.-L. Zhu, Transit. Metal Chem. 36 (2011) 319–324.
[49] B. Krajewska, J. Chem. Technol. Biotechnol. 52 (1991) 157–162.